Improvement of Separation of Polystyrene Particles with PAN Membranes in Hollow Fiber Flow Field-Flow Fractionation

Se-Jong Shin, Hyun-Joo Chung, Byoung-Ryul Min,* Jin-Won Park, Ik-Sung An, and Kangtaek Lee

Department of Chemical Engineering, Yonsei University, Seoul 120-749, Korea
Received May 26, 2003

Hollow Fiber flow field-flow fractionation (HF-FlFFF) has been tested in polyacrylonitrile (PAN) membrane channel in order to compare it with polysulfone (PSf) membrane channel. It has been experimentally shown that the separation time of 0.05-0.304 μm polystyrene latex (PSL) standards in PAN membrane channel is shorter than that in PSf channel by approximately 65%. The optimized separation condition in PAN membrane is V_{out}/V_{rad} = 1.4/0.12 mL/min. which is equal to the condition in PSf membrane channel. In addition both the resolution (R_s) and plate height (H) in PAN membrane channel are better than that in PSf membrane channel. The membrane radius was obtained by back calculation with retention time. It shows that the PSf membrane is expanded by swelling and pressure, but the PAN membrane doesn't expand by swelling and pressure.

Key Words : Hollow fiber, Flow field-flow fractionation, Polyacrylonitrile membrane, Optimized separation condition

Introduction

Field-flow fractionation is a category of separation techniques that fractionate colloidal particles or macromolecules by the use of external fields driven across the direction of separation flow for sample migration.[1] Among the various FFF sub techniques, flow field flow fractionation (flow FFF) is potentially capable of the rapid separation of a wide variety of macromolecular and colloidal materials at high resolution.[2-4]

In 1986 an asymmetrical flow FFF system was developed by two different groups.[5,6] In the system, only one of the channels is permeable for the solvent. The other channel wall is made of float glass to make visual inspection of the processes in the channel possible. However, the result obtained with this channel encouraged a further development of the method. Asymmetric flow FFF is instrumentally simpler than symmetric type, since it requires the less control of one flow-rate. Disadvantage is that the axial and cross flow cannot be chosen independently, and that the axial flow is not constant over the length of the channel. In the third type of flow FFF a microporous hollow fiber is used as the separation channel. Since the radial and axial flow decrease to the axial direction, this type is regarded as asymmetric type.

In 1974 Lee et al. already conducted the study with a bundle of hollow fibers, which can be regarded as flow FFF experiments.[7] In 1989 Jönsson and Carlshaf presented their hollow-fiber flow FFF (HF^5) system.[8] Jönsson and Carlshaf applied the system to separation of polystyrene latex beads studying sample overloading, the influence of ionic strength of the solvent and the properties of various fiber types.[9-11] In 1995 Wijnhoven *et al.* applied the same HF^5 system to separate polystyrene sulfonate and to investigate water-soluble polymers.[12,13]

Recently, it has been reported that particle separation by HF-FlFFF can be greatly improved to the resolution level normally achieved by a rectangular system by optimization.[14] Furthermore it has been shown that hollow fiber can be a potential alternative to obtain particle size distribution provided that it is developed into a facilitated and disposable module in HF-FlFFF. In HF-FlFFF, however, the problem has been raised that PSf membrane is expanded by operation pressure unlike the rectangular channel.

Normally in FFFF, a flat rectangular separation channel consisting of two parallel plates is used. The force field is a secondary flow of liquid (cross flow) going through the two channel walls, transverse to the elution flow. This arrangement requires that both channel walls should be permeable. In most of the cases, the channel walls are membranes made of polysulfone or cellulose-based material with a homogeneously porous "skin-like" surface. For stability this smooth surface is supported by a more rigid and coarse membrane construction. Typical molecular weight cut-off for the membranes used in FFFF is between 5,000 and 100,000.

As opposed to the normal arrangement with two parallel plates for a separation channel in FFFF, a new approach using a cylindrical hollow fiber is presented in this study.

In this study, PAN membrane has been used in HF-FlFFF channel instead of PSf membrane that has been commonly used till now. To compare performance of PAN membrane and PSf membrane, plate height, resolution and recovery of two membranes were investigated. In order to estimate the change in radius, back calculation is made to obtain an expanded radius from the experimental retention data.

Theory

A cylindrical hollow fiber FFF has certain advantages, such as simplicity in operation and independent control of

*Corresponding Author. Tel & Fax: +82-2-365-8570; E-mail: minbr345@yonsei.ac.kr

the two flows (elution and cross flow), including an easier way of performing gradient elution. The cylindrical channel automatically tends to maintain its cylindrical cross section when pressurized. The triangular ends that are present in the classical configuration are avoided. These have been shown to be a possible cause of additional band broadening.

Retention time t_r in HF-FlFFF can be written as: [11,15]

$$t_r = \frac{r_f^2}{8D}\ln(\langle v\rangle(\zeta)/\langle v\rangle(L)) \quad (1)$$

Here, r_f and D are the hollow fiber radius and diffusion coefficient, respectively. $\langle v\rangle(\zeta)$ and $\langle v\rangle(L)$ are the mean axial flows in the beginning and end of the fiber.

If D is expressed by the Stokes-Einstein equation

$$D = \frac{kT}{3\pi\eta d} \quad (2)$$

Here, k, T, η and d are the Boltzmann constant, temperature, carrier solution viscosity and particle diameter, respectively.

Band broadening in FFF systems can be measured by the plate height H, comprised of the following components

$$H = H_D + H_n + \Sigma H_i \quad (3)$$

where H_D is the longitudinal diffusion contribution and H_n is due to non-equilibrium band broadening and ΣH_i is the sum of contributions due to system non-idealities.

Resolution, like separation factor, differs for each specific component pair and therefore fails as global criterion of separation.[16] For analytical separations, more universal criteria have evolved, such as plate height, number of plate, rate of generation plates, and peak capacity. The most important index of success for the analytical separation of two specific components is the resolution R_s. This parameter categorizes the overlap of two specific component zones. If the centers of gravity of the two zones are founded at locations X_1 and X_2, respectively, then the resolution can be defined as[17]

$$R_s = \frac{2(X_2 - X_1)}{W_{b1} + W_{b2}} \quad (4)$$

where X is the peak retention volume; W_b is the peak width formed by intersection of the tangents to the curve inflection points with the baseline in retention volume units, $W_b = 4\sigma$ and σ is the peak standard deviation (proportional to peak width).

The subscripts 1 and 2 serve to identify two closely eluting solutes. The plate height H is equal to L/N, where L is the column length.

Eq. (4) may also be written as

$$R_s = \frac{X_2 - X_1}{2(\sigma_1 + \sigma_2)} \quad (5)$$

Exprimental Section

Apparatus and Chemicals. The HF-FlFFF system configuration is represented in Figure 1. The hollow fibers used in this work are PAN having a molecular weight cut-off of 50,000 obtained from SAMBO (Korea), and PSf having a molecular weight cut-off of 30,000 obtained from SKU (Seoul, Korea). The hollow fiber separation module is prepared in the same way as described in the previous work.[14] The dimensions of the PAN fiber are 24 cm in length (L) and 0.415 mm (in dried condition) of radius (r_f). The dimensions of which fiber is 24.0 cm in length (L) and 0.40 mm (in dried condition) of radius (r_f). In the case of PSf membrane, the actual radius of the fiber is back calculated by using Eq. (1). It is 0.46 mm since an expansion of fiber somehow occurs due to the system pressure during running. The fiber is encapsulated in a 1/8 inch empty teflon tube (0.078 inch in i.d.) and both ends of the fiber are fixed to the inner wall of the teflon tube with epoxy glue.

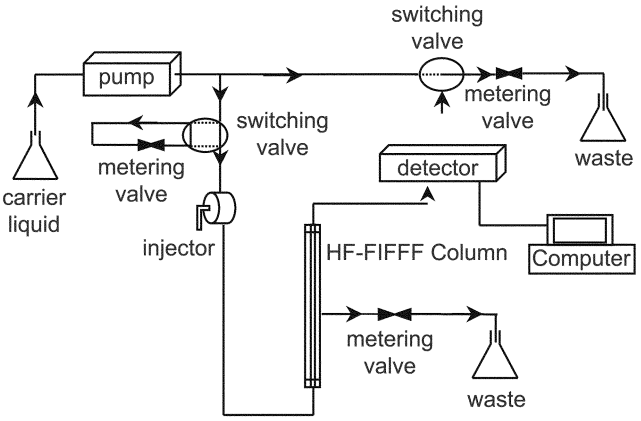

Figure 1. Illustration of HF-FlFFF system. the indicated flow direction and valve positions are for opposing flow relexation and focusing. Solid lines indicated valve positions during elution.

The carrier solution is prepared by ultra pure water containing 0.1% FL-70 (Fisher Scientific, USA) for particle dispersion and 0.02% NaN_3 (sodium azide) as bactericide. The solution is vacuum degassed prior to use and during the run. The sample injection is made at a reduced flow rate (0.5 mL/min) through the inlet of the fiber with the use of a 6 port injection valve (Upchurch Scientific, USA) with the use of a Rheodyne 7125 loop. Carrier solution is delivered to the hollow fiber by an HPLC pump (Younglin Instrument, Korea). Since the current HF-FlFFF system utilizes a single pump, the flow conversion during the focusing/relaxation process is made by using both four-way and three-way switching valves as depicted in Figure 1. Flow rates required for focusing/relaxation are adjusted with a model SS-SS2-VH Nupro metering valve (Nupro, USA). Followed by the sample injection, the focusing/relaxation process is carried out by delivering the carrier liquid into both the fiber inlet and outlet. The focusing process is accomplished with a single pump by splitting the flow into two parts (delivered to both inlet and outlet). The control of flow rates for both ends is made with the use of a model SS-SS2-VH Nupro metering valve which is pre-adjusted to give required flow rates for focusing/relaxation. The flow rate adjustment for the outflow

and radial flow is made with the same metering valve. The sample particles used are polystyrene latex (PSL) standards having nominal diameters of 50, 135, 204 and 304 nm (Duke Scientific, USA). Injection amount of standard samples is about 0.02 μg of each size. Eluted particles are monitored by a Model M720 UV detector from Younglin Instrument. The detector signal is collected by using the Autochro-Win software program from Younglin.

Operating Conditions. The sample is injected at injection period. The sample is injected at a relatively low axial flow rate into the fiber inlet and transported to a focusing point in the fiber.

At the relaxation period the injected sample is relaxed. During this period the pump flow is divided for focusing, so the ratio between the inlet flow and reverse flow determines focusing location. Consequently, the direction of the axial flow at the end of the fiber will reverse and meet the inlet flow. In the point where the total axial flow is zero, the sample is axially compressed by the two opposing flows ($\dot{V}_{in}$, $-\dot{V}_{out}$, minus means opposite direction) and the particles migrate to an equilibrium position close to the wall. The axial location of this relaxation point is governed by the ratio ($\dot{V}_{in}/-\dot{V}_{out}$) and the time needed to transport the solute to the wall depends on the magnitude of the radial flow and the fiber radius.

In the analysis period the axial flow is increased to elution conditions while the radial flow is still maintained at the same rate. The final period is the elution state. In this state, the radial flow is kept unchanged, and the pump flow is maintained as isocratic mode.

Results and Discussion

Separation and Resolution. Figure 2 shows the separation of polystyrene latex mixtures obtained at three different radial flow rate conditions (from 0.1-0.15 mL/min) by PSf membrane HF-FlFFF. All runs are made at $\dot{V}_{out}$ = 1.4 mL/min at room temperature. At radial flow rate, $\dot{V}_{rad}$ = 0.1 mL/min, the peaks are not clearly separated. But when the radial flow rate is elevated to 0.12 mL/min, all peaks are clearly separated. It seems that the resolution of peaks is decreased with further elevation (0.15 mL/min) in radial flow. This is due to the increase of the experimental retention ratio, which results in the increase of the non-equilibrium band broadening in the FFF procedure.

Figure 3 shows the separation of polystyrene latex mixtures obtained at three different radial flow rate conditions (from 0.1-0.15 mL/min) by PAN membrane HF-FlFFF. All conditions are the same as PSf membrane channel. The separation behavior seems that the PAN membrane HF-FlFFF is similar to the PSf membrane.

When the retention times of two membrane channels are compared, the retention time in the PAN membrane HF-FlFFF channel is shorter than that in the PSf membrane HF-FlFFF channel. Also, separation is clearly excellent in the

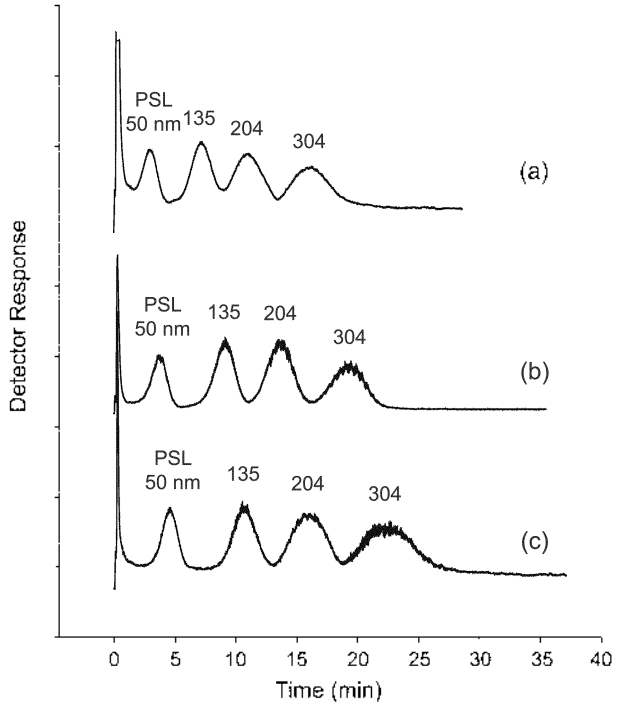

Figure 2. Fractograms of polystyrene separation obtained by PSf membrane HF-FlFFF channel at three different cross flow rates; (a) $\dot{V}_{rad}$ 0.1 mL/min, (b) $\dot{V}_{rad}$ 0.12 mL/min, (c) $\dot{V}_{rad}$ 0.15 mL/min. All runs are obtained at the same out flow rate condition $\dot{V}_{out}$ = 1.4 mL/min.

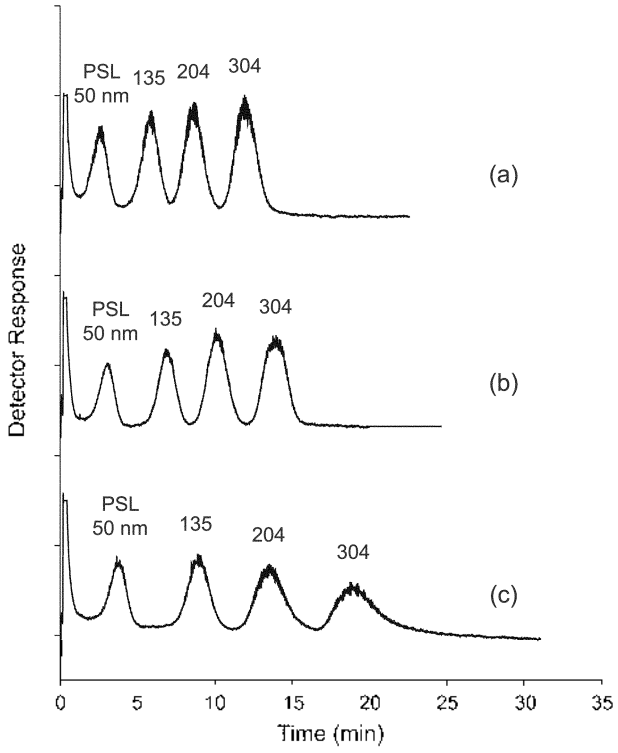

Figure 3. Fractograms of polystyrene separation obtained by PAN membrane HF-FlFFF channel at three different cross flow rates; (a) $\dot{V}_{rad}$ = 0.1 mL/min, (b) $\dot{V}_{rad}$ = 0.12 mL/min, (c) $\dot{V}_{rad}$ = 0.15 mL/min. All runs are obtained at the same out flow rate condition $\dot{V}_{out}$ = 1.4 mL/min.

Table 1. Resolution of three different PSL particle pairs

$\dot{V}_{rad}$	Between 50 and 135 nm		Between 135 and 204 nm		Between 204 and 304 nm	
	PSf	PAN	PSf	PAN	PSf	PAN
0.1 mL/min	1.53	1.57	1.79	1.88	1.93	2.08
0.12 mL/min	1.07	1.26	1.20	1.51	1.18	1.46
0.15 mL/min	0.98	1.38	1.14	1.50	0.89	1.26

PAN membrane channel.

The elution time for all particles is 15 min in the PAN membrane channel against 23 min in the PSf membrane channel.

Table 1 shows the resolution *vs.* radial flow rate for all runs is $\dot{V}_{out}$ = 1.4 mL/min. The resolutions are calculated between 50 and 135 nm PSL particles, between 135 and 204 nm PSL particles, and between 204 and 304 nm PSL particles. The most important index of success for the analytical separation of two specific components is the resolution R_s. The two peaks are clearly separated. The resolution R_s is more than 1.5 when the peak is a Gaussian peak.

The resolution of the PSf membrane is 1.07-1.20 between 135 and 204 nm PSL particles. It means that the peaks are not clearly separated in PSf membrane. But, the resolution of the PAN membrane is 1.26-1.59 between 135 and 204 nm PSL particles. When the radial flow rate condition is 0.12-0.14 mL/min, the resolution is more than 1.5. Under these conditions, the mixture is completely separated. Moreover, at all conditions the resolution of PAN membrane is more than the largest resolution of PSf membrane. The optimized separation condition is $\dot{V}_{out}/\dot{V}_{rad}$ = 1.4/0.15 mL/min.

Plate Height. The experimentally obtained plate heights are shown in Figure 4-7. The experimental plate height data are plotted against the radial flow rate for 50 nm PSL particle in Figure 4 and 204 nm in Figure 5. In Figure 4 the plate height becomes smaller as the radial flow rate becomes larger. But, the tendency between the plate height and the radial flow rate appears to vary in Figure 5. It is believed that the main reason of discrepancy is the initial distribution of the sample. The plate height is fatally influenced by the peak standard deviation. The theoretical peak deviation is derived under the condition, in which the initial sample distribution is regarded as delta function. In experiments, the initial sample at the end of relaxation seems not to be arranged like delta function. The peak standard deviation increases by this broadening of initial sample zone. This results in an increased plate height. A similar result was already reported at the rectangular channel by Wahlund.[6]

Nevertheless in Figure 4-7 the plate height of the PAN membrane channel is smaller than that of PSf membrane channel. It is one set of evidence that the performance of the PAN membrane channel is better than that of the PSf

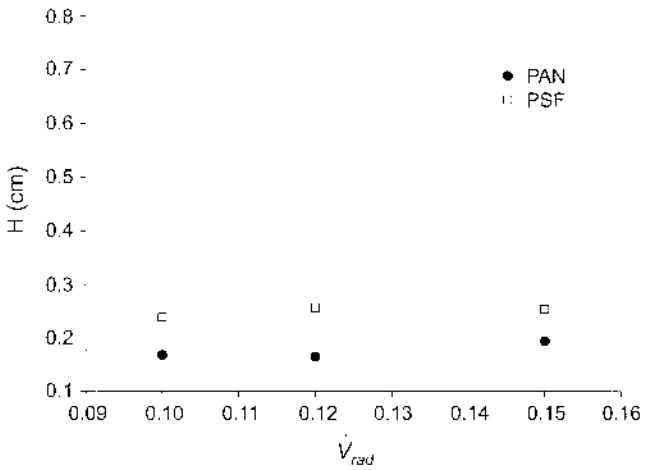

Figure 5. The measured plate heights *vs.* $\dot{V}_{rad}$ for 204 nm PSL particle in the PSf and the PAN membrane HF-FIFFF channel.

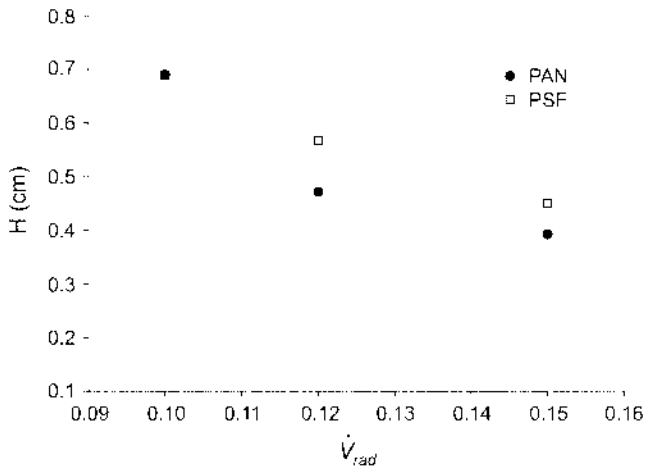

Figure 4. The measured plate heights *vs.* $\dot{V}_{rad}$ for 50 nm PSL particle in the PSf and the PAN membrane HF-FIFFF channel.

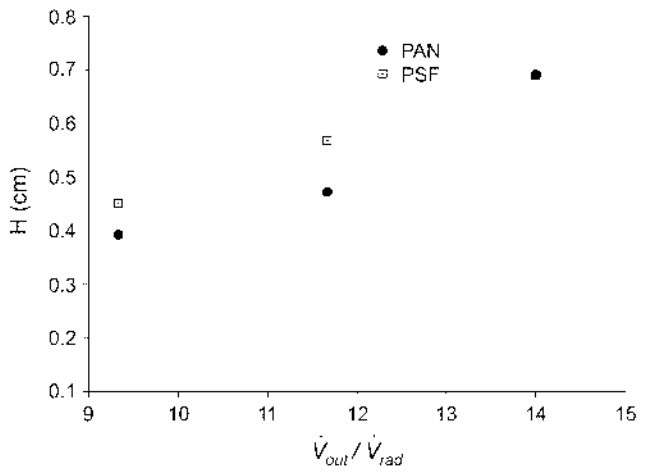

Figure 6. The measured plate heights *vs.* $\dot{V}_{out}/\dot{V}_{rad}$ for 50 nm PSL particle in the PSf and the PAN membrane HF-FIFFF channel.

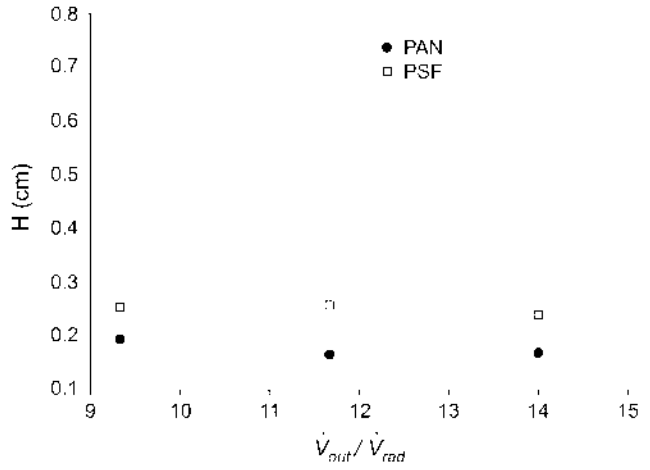

Figure 7. The measured plate heights *vs.* $\dot{V}_{out}/\dot{V}_{rad}$ for 204 nm PSL particle in the PSf and the PAN membrane HF-FIFFF channel.

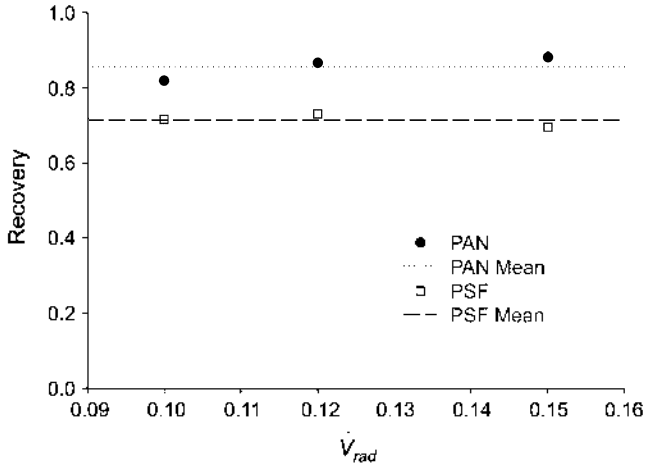

Figure 8. The recovery of 50 nm PSL particle in two different membrane HF-FIFFF channels.

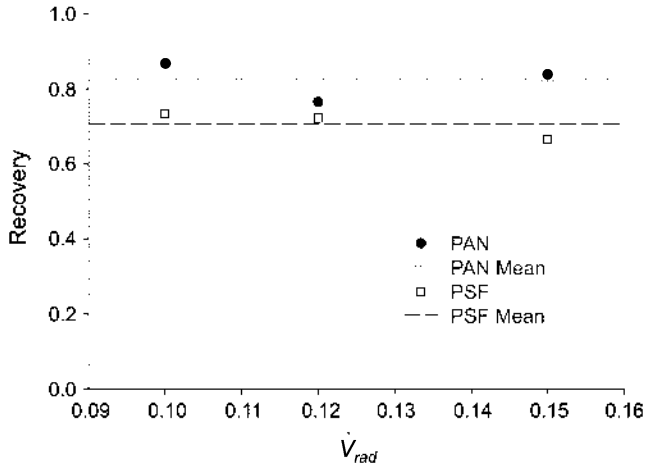

Figure 9. The recovery of 204 nm PSL particle in two different membrane HF-FIFFF channels.

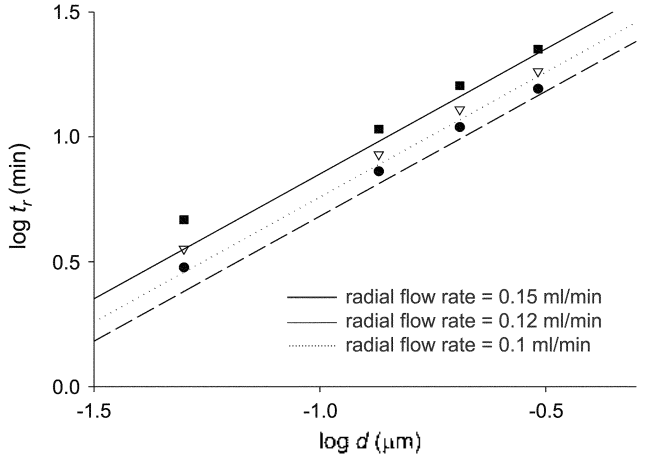

Figure 10. Plot of log t_r *vs.* log d of PSL particles obtained in the PSf membrane channel at different axial flow rate conditions. For all runs it is $\dot{V}_{in}$ = 1.4 mL/min. The radial flow rates of each set of data are ■ ($\dot{V}_{rad}$ = 0.1 mL/min), ▽ ($\dot{V}_{rad}$ = 0.12 mL/min) and ● ($\dot{V}_{rad}$ = 0.15 mL/min) and the linear lines are calculated with the basis of each calibrated radius from four PSL particles (50, 135, 204, 304 nm).

membrane channel.

Recovery. Figure 8 and 9 show the recovery of the PSf membrane channel and the PAN membrane channel by 50 and 204 nm PSL particles respectively. It has been found that the recovery range by 50 nm PSL particle in the PSf membrane channel is 0.67-0.73 and the recovery range in the PAN membrane channel is 0.77-0.87 (Figure 8). It is also clear from Figure 9 that the recovery range in the PSf membrane channel is 0.7-0.73 and the recovery range in the PAN membrane channel is 0.78-0.87 by 204 nm PSL particle.

On the whole, recovery of PSL particle in the HF-FIFFF channel becomes smaller as is increased. It is believed that sample is accumulated in the accumulation wall or escapes by pore because distance between the sample and the accumulation wall approaches according as radial flow rate increases.

Retention Behavior. As particle diameter decreases, the distance from the wall increases. This means that the elution of low particle is faster than the large one.

Particle retention in HF-FIFFF is examined by comparing experimental retention time with the theory in Eq. (1), an accurate knowledge of efficient fiber radius must be known first.

Figure 10 and 11 are the plot of log t_r *vs.* log d of PSL standards obtained in PSf and PAN membrane channel, respectively. The solid, dash and dotted lines represent the semi-empirical theory value of each run conditions. The data points for the large diameter size appear to be deviated from the expected value, which may be due to a steric influence.

Conclusions

In the present work, we experimentally compared the performance of a hollow fiber membrane PSf and PAN for the separation of polystyrene latex standards in the Flow FFF. This work presents the theory that using the PAN membrane channel instead of the PSf membrane, which is

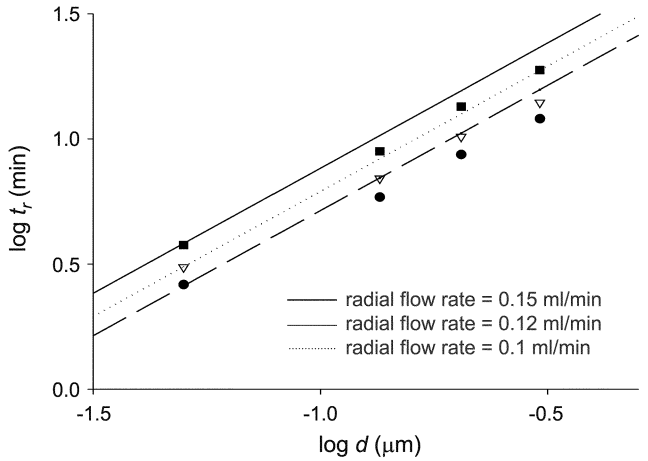

Figure 11. Plot of log t_r *vs.* log d of PSL particles obtained in PAN membrane channel at different axial flow rate conditions. For all runs it is $\dot{V}_{in}$ = 1.4 mL/min. The radial flow rates of each set of data are ■ ($\dot{V}_{rad}$ = 0.1 mL/min), ▽ ($\dot{V}_{rad}$ = 0.12 mL/min), ● ($\dot{V}_{rad}$ = 0.15 mL/min) and the linear lines are calculated with the basis of each calibrated radius from four PSL particles (50, 135, 204, 304 nm).

used widely as FFF column, is expanded under the pressure given by the system.

The elution time of the PAN membrane channel is found to be shorter than that of the PSf membrane channel. From this point of view, the elution time of the mixture sample in the PAN membrane channel is 15 min at radial flow rate 0.12 mL/min, but in the PSf membrane channel it is 23 min. It is also found that the resolution of PAN membrane channel is better than that of PSf membrane channel. Resolution ranges of PAN and PSf membrane channel are 1.26-1.59 and 1.07-1.20 respectively.

The optimized separation condition in the PAN membrane channel is $\dot{V}_{out}/\dot{V}_{rad}$ = 1.4/0.12 mL/min. It is equal to optimized separation condition in the PSf membrane channel.

Plate height in PAN membrane channel is also found to be smaller than that in PSf membrane. The recovery of 50 and 204 nm PSL particles in PAN membrane is 0.77-0.87 but in PSf membrane it is 0.67-0.73.

Experimentally determined retention time of the PSf membrane channel is larger than the theoretical value because of expansion of PSf membrane by pressure and swelling. But since this is similar to theoretical value in PAN membrane channel, it shows that it is not expanded or swelled under pressure. Therefore in this study, it has been found that PAN membrane is superior to PSf membrane in point of performance and structural character.

Acknowledgments. This work was supported by grant No. R01-2001-000-00420-0 from the Korea Science & Engineering Foundation.

References

1. Giddings, J. C. *Science* **1993**, *260*, 1456.
2. Giddings, J. C. *Anal. Chem.* **1981**, *53*, 1170A.
3. Janca, J. *Field-Flow Fractionation: Analysis of Macromolecules and Particles (Chromatographic Science Series)*; Marcel Dekker: New York, U. S. A., 1987; Vol. 39.
4. Caldwell, K. D. *Anal. Chem.* **1988**, *60*, 959A.
5. Granger, J.; Dodds, J.; Leclerc, D.; Midoux, N. *Chem. Eng. Sci.* **1986**, *41*, 3119.
6. Walund, K. G.; Giddings, J. C. *Anal. Chem.* **1987**, *59*, 1332.
7. Lee, H. L.; Reis, J. F. G.; Dohner, J.; Lightfoot, E. N. *AIChE. J.* **1974**, *20*, 776.
8. Jönsson, J. Å.; Carlshaf, A. *Anal. Chem.* **1989**, *61*, 11.
9. Carlshaf, A.; Jönsson, J. Å. *Sep. Sci. Tech.* **1993**, 1191.
10. Carlshaf, A.; Jönsson, J. Å. *J. Microcol. Sep.* **1991**, *3*, 411.
11. Carlshaf, A.; Jönsson, J. Å. *Sep. Sci. Tech.* **1993**, *28*, 1031.
12. Wijnhoven, J. E. G. J.; Koon, J. P.; Poppe, H.; Kok, W. T. *J. Chromatogr.* **1995**, *699*, 119.
13. Wijnhoven, J. E. G. J.; Koon, J. P.; Poppe, H.; Kok, W. T. *J. Chromatogr.* **1996**, *732*, 307.
14. Lee, W. J.; Min, B. R.; Moon, M. H. *Anal. Chem.* **1999**, *71*, 3449.
15. Janka, J.; Chmelik, J.; Pribylova, D. *J. Liq. Chromatogr.* **1985**, *8*, 2343.
16. Giddings, J. C. *Unified Separation Science*; Wiley-Interscience: New York, U. S. A., 1991.
17. Yau, W. W.; Kirkland, J. J.; Bly, D. D. *Modern Size-Exclusion Liquid Chromatography*; Wiley-Interscience: New York, U. S. A., 1979.
18. Williams, P. S.; Moon, M. H.; Xu, Y.; Giddings, J. C. *Chem. Eng. Sci.* **1996**, *51*, 4477.
19. Williams, P. S.; Kosh, T.; Giddings, J. C. *Chem. Eng. Column.* **1992**, *111*, 121.
20. Williams, P. S.; Lee, S.; Giddings, J. C. *Chem. Eng. Column.* **1994**, *130*, 143.
21. Williams, P. S.; Moon, M. H.; Giddings, J. C. *Particle Size Analysis*; Stanly-Wood, N. G.; Line, R. W., Eds.; Springer Verlag: Berlin, Germany, 1992.